Journal of Engineering Physics and Thermophysics, Vol. 65, No. 6, 1993

IDENTIFICATION OF NONSTEADY HEAT FLUXES BY USING THE OUTPUT SIGNALS OF THIN-MEMBRANE GARDON-TYPE SENSORS

A. M. Vorob'ev, V. I. Zhuk,
V. P. Sizov, and D. N. Chubarov

UDC 536.084.2

An operator comparing the nonsteady output signals of a sensor to the characteristics of an external thermal perturbation is constructed.

Thin-membrane sensors of heat flux density are used to investigate the intensity of heat transfer in various elements of equipment in both full-scale and model experiments.

Structurally, the sensor is a thin Constantan foil welded around the periphery of the cross section of a hollow cylinder (Fig. 1). Taken together, the elements of the sensor form two copper-Constantan thermocouples: one at the center and the other at the edge of the membrane. The difference in emf of the two thermocouples, which is the output signal of the sensor, may evidently be compared with some intensity characteristics of an external thermal perturbation using some operator. In the situation where the heat flux supplied is uniformly distributed over the membrane radius, the difference in emf is directly proportional to the heat flux density in steady conditions. With standard calibration of the given sensors by means of radiative heating, the sensor itself emits a relatively small radiant flux, and therefore the temperature gradient along the membrane does not play a significant role in the heat transfer by radiation.

The use of sensors of the given type with calibration characteristics obtained on heating by radiant fluxes under conditions of convective heat transfer may lead, as shown in [1-3], to substantial errors because of the significant temperature gradients along the membrane.

In [1-3], recommendations are given, based on the investigations performed, that allow for the nonlinearity of the calibration characteristics under conditions of combined heat transfer. The situation evidently becomes much more complicated when such sensors are used under nonsteady conditions. For a correct interpretation of the measurement data in this case, it is necessary to analyze the properties of a thermal model of the sensor with an account for the set of factors influencing the formation of a nonsteady temperature field in structural elements of the sensor. Indeed, without such investigations, it is difficult to judge what actual characteristics of heat transder intensity are measured by these sensors. From a priori considerations, it may simply be assumed that the measurable emf difference evidently corresponds to some integral (relative to the time and the membrane surface) characteristics of the thermal perturbation.

For analysis of the sensor behavior under nonsteady conditions, we consider a thermal model of the sensor (Fig. 1), including a thin membrane in ideal thermal contact over its periphery with the end of a hollow copper cylinder. It is assumed that the radius ratio $R_{\mathrm{in}0}/R_{\mathrm{out}}$ (see Fig. 1) allows the temperature field in the cylinder to be regarded as one-dimensional; the temperature difference over the membrane thickness is neglected.

The thermal model of the sensor accounts for heat losses through the central electrode as well as those from the membrane and the lateral faces of the peripheral electrode. The heat flux supplied to the membrane is assumed to be symmetrical relative to the sensor axis and to change arbitrarily over the radius; the heat-flux distribution in the contact zone of the membrane with the cylinder is assumed to be uniform.

The mathematical model in this case is described by the following system of heat-conduction equations and boundary and initial conditions:

Translated from Inzhenerno-Fizicheskii Zhurnal, Vol. 65, No. 6, pp. 718-724, December, 1993.

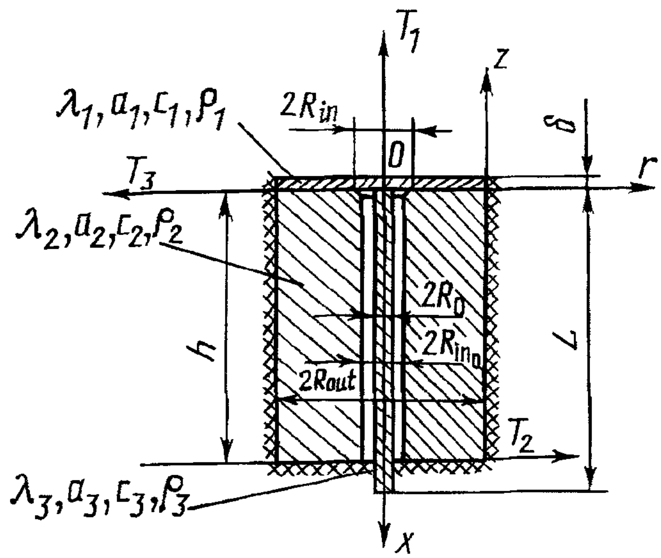

Fig. 1. Thermal model of the sensor.

$$\frac{\partial^2 T_1(\bar{r}, \mathrm{Fo})}{\partial \bar{r}^2} + \frac{1}{\bar{r}} \frac{\partial T_1(\bar{r}, \mathrm{Fo})}{\partial \bar{r}} - \beta_1 T_1(\bar{r}, \mathrm{Fo}) + \bar{q}(\bar{r}, \mathrm{Fo}) = \frac{\partial T_1(\bar{r}, \mathrm{Fo})}{\partial \mathrm{Fo}}, \tag{1}$$

$$\frac{\partial^2 T_2(\bar{z}, \mathrm{Fo})}{\partial \bar{z}^2} - \beta_2 T_2(\bar{z}, \mathrm{Fo}) = k_2 \frac{\partial T_2(\bar{z}, \mathrm{Fo})}{\partial \mathrm{Fo}}, \tag{2}$$

$$\frac{\partial^2 T_3(\bar{x}, \mathrm{Fo})}{\partial \bar{x}^2} - \beta_3 T_3(\bar{x}, \mathrm{Fo}) = k_3 \frac{\partial T_3(\bar{x}, \mathrm{Fo})}{\partial \mathrm{Fo}}, \tag{3}$$

$$\gamma_2 \frac{\partial T_2(\bar{z}, \mathrm{Fo})}{\partial \bar{z}}\bigg|_{\bar{z}=h} = \bar{q}(1, \mathrm{Fo}) - \frac{\partial T_1(1, \mathrm{Fo})}{\partial \mathrm{Fo}} - \varepsilon_2 \frac{\partial T_1(\bar{r}, \mathrm{Fo})}{\partial \bar{r}}\bigg|_{\bar{r}=1}, \tag{4}$$

$$T_2(\bar{h}, \mathrm{Fo}) = T_1(1, \mathrm{Fo}); \quad \frac{\partial T_2(\bar{z}, \mathrm{Fo})}{\partial \bar{z}}\bigg|_{\bar{z}=0} = 0, \tag{5}$$

$$-\gamma_3 \frac{\partial T_3(\bar{x}, \mathrm{Fo})}{\partial \bar{x}}\bigg|_{\bar{x}=0} = \bar{q}(\bar{R}_0, \mathrm{Fo}) - \frac{\partial T_1(\bar{R}_0, \mathrm{Fo})}{\partial \mathrm{Fo}} + \varepsilon_3 \frac{\partial T_1(\bar{r}, \mathrm{Fo})}{\partial \bar{r}}\bigg|_{\bar{r}=\bar{R}_0}, \tag{6}$$

$$T_3(0, \mathrm{Fo}) = T_1(\bar{R}_0, \mathrm{Fo}), \quad \frac{\partial T_3(\bar{x}, \mathrm{Fo})}{\partial \bar{x}}\bigg|_{\bar{x}=\bar{L}} = 0. \tag{7}$$

The initial temperature of the system is assumed equal to zero, i.e., $T_1(\bar{r}, 0) = T_2(\bar{z}, 0) = T_3(\bar{x}, 0) = 0$.

In the above model the nonuniformity of the temperature fields over the sections of the electrode at the periphery and the central electrode is ignored. For generality of the problem, the thermophysical characteristics of the electrode at the periphery and the central electrode are assumed to be different (in reality $\lambda_2 = \lambda_3$, $a_2 = a_3$). The temperature of the medium participating in heat transfer with the internal surfaces of the sensor parts is assumed to be equal to the initial temperature of the system, i.e., $T_s = 0$.

Using the Laplace transformation with respect to time (the variable Fo) a solution to the system of equations (1)-(3) may be written in the form

$$T_1(\bar{r}, s) = A_1 I_0(\sqrt{s+\beta_1}\,\bar{r}) + B_1 K_0(\sqrt{s+\beta_1}\,r) + \tag{8}$$

$$+ \int_{R_0}^{\bar{r}} \xi \bar{q}(\xi, s)\,[I_0(\sqrt{s+\beta_1}\,\xi) K_0(\sqrt{s+\beta_1}\,\bar{r}) - I_0(\sqrt{s+\beta_1}\,\bar{r}) K_0(\sqrt{s+\beta_1}\,\xi)]\,d\xi\,;$$

$$T_2(\bar{z}, s) = A_2 \operatorname{ch}(\sqrt{s+\beta_2}\,k_2^{1/2}\bar{z}) + B_2 \operatorname{sh}(\sqrt{s+\beta_2}\,k_2^{1/2}\bar{z})\,; \tag{9}$$

$$T_3(\bar{x}, s) = A_3 (\operatorname{ch}(\sqrt{s+\beta_3}\,k_3^{1/2}\bar{x}) + B_3 \operatorname{sh}(\sqrt{s+\beta_3}\,k_3^{1/2}\bar{x})\,, \tag{10}$$

where $I_0(\xi)$, $K_0(\xi)$ are the modified Bessel function and the MacDonald function, respectively; s is the parameter of the Laplace transformation.

With an account for the boundary and initial conditions and assuming that $\bar{q}(\bar{r}, s) = \bar{q}(\bar{R}_0, s) + \Delta\bar{q}(\bar{r}, s)$, where $\bar{q}(\bar{R}_0, s)$ is the density of the heat flux supplied to the membrane near the central electrode, we have in the Laplace transforms

$$q(\bar{R}_0, s) + \Delta q(s) = \frac{\lambda_1 \delta}{R_{\text{in}}^2}\, s\,[\varphi_1(s) + \varphi_2(s) + \varphi_3(s)]\,, \tag{11}$$

where

$$\varphi_1(s) = \Delta T(s) \frac{\tilde{\varphi}_0(s) + \bar{R}_0/\varepsilon_3\,[s + \sqrt{s}\,k_3^{1/2}\gamma_3 \operatorname{th}(\sqrt{s}\,k_3^{1/2}\bar{L})]\,\tilde{\varphi}_1(s)}{\psi(s)}\,; \tag{12}$$

$$\varphi_2(s) = \varphi_1(s) \frac{\sqrt{s}\operatorname{cth}(\sqrt{s}\,k_2^{1/2}\bar{h})}{\gamma_2 k_2^{1/2}}\,; \tag{13}$$

$$\varphi_3(s) = \frac{\varepsilon_2 \operatorname{cth}(\sqrt{s}\,k_2^{1/2}\bar{h})}{\gamma_2 k_2^{1/2}\psi(s)} \left[\tilde{\varphi}_2(s) + \frac{\sqrt{s}\,\bar{R}_0}{\varepsilon_3}(s + \sqrt{s}\,\gamma_3 k_3^{1/2} \operatorname{th}(\sqrt{s}\,k_3^{1/2}\bar{L}))\,\tilde{\varphi}_3(s)\right] \Delta T(s)\,; \tag{14}$$

$$\tilde{\varphi}_0(s) = \sqrt{s}\,\bar{R}_0\,[I_0(\sqrt{s}) K_1(\sqrt{s}\,\bar{R}_0) + K_0(\sqrt{s}) I_1(\sqrt{s}\,\bar{R}_0)]\,;$$

$$\tilde{\varphi}_1(s) = I_0(\sqrt{s}) K_0(\sqrt{s}\,\bar{R}_0) - I_0(\sqrt{s}\,\bar{R}_0) K_0(\sqrt{s})\,;$$

$$\tilde{\varphi}_2(s) = \bar{R}_0\, s\,[I_1(\sqrt{s}) K_1(\sqrt{s}\,\bar{R}_0) - I_1(\sqrt{s}\,\bar{R}_0) K_1(\sqrt{s})]\,;$$

$$\tilde{\varphi}_3(s) = K_0(\sqrt{s}\,\bar{R}_0) I_1(\sqrt{s}) + K_1(\sqrt{s}) I_0(\sqrt{s}\,\bar{R}_0)\,;$$

$$\psi(s) = \sqrt{s}\,\bar{R}_0\,[I_0(\sqrt{s}) K_1(\sqrt{s}\,\bar{R}_0) + K_0(\sqrt{s}) I_1(\sqrt{s}\,\bar{R}_0)] - \frac{\varepsilon_2}{\varepsilon_3}\bar{R}_0\sqrt{s}\,\times$$

$$\times \frac{\gamma_3 k_3^{1/2}}{\gamma_2 k_2^{1/2}} \frac{\operatorname{th}(\sqrt{s}\,k_3^{1/2}\bar{L})}{\operatorname{th}(\sqrt{s}\,k_2^{1/2}\bar{h})} [K_1(\sqrt{s}) I_0(\sqrt{s}\,\bar{R}_0) + I_1(\sqrt{s}) + K_0(\sqrt{s}\,\bar{R}_0)] +$$

$$+\frac{\overline{R}_0 s}{\varepsilon_3}\left[1-\frac{\gamma_3 k_3^{1/2}\,\mathrm{th}\,(\sqrt{s}\,k_3^{1/2}\overline{L})}{\gamma_2 k_2^{1/2}\,\mathrm{th}\,(\sqrt{s}\,k_2^{1/2}\overline{h})}\right][I_0(\sqrt{s})\,K_0(\sqrt{s}\,\overline{R}_0)-$$

$$-I_0(\sqrt{s}\,\overline{R}_0)\,K_0(\sqrt{s})]-\left[1-\frac{\varepsilon_2}{\varepsilon_3}\overline{R}_0\frac{k_3^{1/2}\gamma_3\,\mathrm{th}\,(\sqrt{s}\,k_3^{1/2}\overline{L})}{k_2^{1/2}\gamma_2\,\mathrm{th}\,(\sqrt{s}\,k_2^{1/2}\overline{h})}\right];$$

$\Delta q(s)$ is the component of the external thermal perturbation caused by the nonuniformity of the heat-flux distribution with respect to the membrane radius (its form is not given because of the unwieldy expression), $\alpha_1 = \alpha_2 = \alpha_3 = 0$.

In the situation where $\lambda_2 = \lambda_3 = \lambda_e$, $a_2 = a_3 = a_e$, $c_2 = c_3 = c_e$, $\rho_2 = \rho_3 = \rho_e$ and, moreover, $\overline{R}_0$ is small and h, L are sufficiently large (or Fo is small), the following approximations are valid for φ_1, φ_2, φ_3:

$$\varphi_1(s) \simeq \Delta T(s)\,\overline{\overline{\psi}}(s)+\frac{1}{4}\left(\frac{R_0}{R_{\mathrm{in}}}\right)^2\Delta T(s)\,sK_0(\sqrt{s}\,\overline{R}_0)\,\overline{\overline{\psi}}(s)+ \tag{15}$$

$$+\left(\frac{\lambda_e c_e \rho_e}{\lambda_m c_m \rho_m}\right)^{1/2}\frac{1}{2}\frac{R_0}{\delta}\frac{R_0}{R_{\mathrm{in}}}\Delta T(s)\sqrt{s}\,K_0(\sqrt{s}\,\overline{R}_0)\,\overline{\overline{\psi}}(s);$$

$$\varphi_2(s) \simeq \left(\frac{\lambda_m c_m \rho_m}{\lambda_e c_e \rho_e}\right)^{1/2}\frac{\delta}{R_{\mathrm{in}}}\sqrt{s}\,\varphi_1(s); \tag{16}$$

$$\varphi_3(s) \simeq \left(\frac{\lambda_m c_m \rho_m}{\lambda_e c_e \rho_e}\right)^{1/2}\frac{\delta R_0}{R_{\mathrm{in}}^2}\{\varepsilon_2\,\Delta T(s)\,K_1(\sqrt{s}\,\overline{R}_0)\,\overline{\overline{\psi}}_1(s)+$$

$$+\varepsilon_2/\varepsilon_3\,\Delta T(s)\,sK_0(\sqrt{s}\,\overline{R}_0)\,\overline{\overline{\psi}}_1(s)\}+\frac{\delta}{R_{\mathrm{in}}}\frac{R_0}{R_{\mathrm{in}}}\frac{\varepsilon_2}{\varepsilon_3}\Delta T(s)\sqrt{s}\,K_0(\sqrt{s}\,R_0)\,\overline{\overline{\psi}}_1(s); \tag{17}$$

$$\overline{\overline{\psi}}(s)=1+\left[\frac{\varepsilon_2}{\varepsilon_3}\overline{R}_0\frac{\sqrt{s}\,I_1(\sqrt{s})}{I_0(\sqrt{s})}K_0(\sqrt{s}\,\overline{R}_0)+\frac{1-\overline{R}_0\,\varepsilon_2/\varepsilon_3}{I_0(\sqrt{s})}\right]+$$

$$+\left[\frac{\varepsilon_2}{\varepsilon_3}\overline{R}_0\frac{\sqrt{s}\,I_1(\sqrt{s})}{I_0(\sqrt{s})}K_0(\sqrt{s}\,\overline{R}_0)+\frac{1-\overline{R}_0\,\varepsilon_2/\varepsilon_3}{I_0(\sqrt{s})}\right]^2+\ldots;$$

$$\overline{\overline{\psi}}_1(s)=\frac{I_1(\sqrt{s})}{I_0(\sqrt{s})}\psi(s),\quad \lambda_m=\lambda_1,\quad a_m=a_1,\quad c_m=c_1,\quad \rho_m=\rho_1.$$

The inverse transforms were obtained using well-known inversion theorems and tables for integral Laplace transformation [4, 5]. When developing the numerical algorithms, we used the following approximation for convolution of the functions:

$$F_1 * F_2=\int_0^{\mathrm{Fo}}F_1(\mathrm{Fo}-\vartheta)\,F_2(\vartheta)\,d\vartheta=F(\mathrm{Fo}),$$

$$F(n\Delta\mathrm{Fo})=\frac{1}{2}\sum_{i=1}^{n}\left\{F_1[(n-i+1)\Delta\mathrm{Fo}]+F_1[(n-i)\Delta\mathrm{Fo}]\right\}\times$$

$$\times \left\{ \int_0^{i\Delta \mathrm{Fo}} F_2(\vartheta)\, d\vartheta - \int_0^{(i-1)\Delta \mathrm{Fo}} F_2(\vartheta)\, d\vartheta \right\}.$$

Next, a program for a computer was developed to determine the nonsteady values

$$\tilde{q}_0(\mathrm{Fo}) \equiv q(\overline{R}_0,\ \mathrm{Fo}) + \Delta q(\mathrm{Fo}) = \frac{\lambda_1 \delta}{R_{\mathrm{in}}^2} \frac{d}{d\mathrm{Fo}} (\varphi_1 + \varphi_2 + \varphi_3) \tag{18}$$

from the measured ΔT values corresponding to the temperature differences of the membrane near the central electrode and the electrode at the periphery. The program also allows calculation of the difference $\Delta \tilde{q}_0 = \tilde{q}_0(\mathrm{Fo}) - q_{\mathrm{st}}(\mathrm{Fo})$, where q_{st} is the heat flux determined by means of standard calibration characteristics. Obviously, when $\Delta \tilde{q}_0$ is small, the data obtained using the standard calibration characteristics may be recognized as reliable; otherwise the reliability of the $\tilde{q}_0(\mathrm{Fo})$ measurement data from use of the standard calibration is rather doubtful. The program developed was tested in a numerical experiment in which the results of solution of some direct problems on heating of the sensor components by a nonsteady convective heat flux, supplied to the membrane surface, were used as the initial data (as regards ΔT). As judged from the results of this experiment, the calculation algorithms developed, which ensure good agreement between the calculated $\tilde{q}_0(\mathrm{Fo})$ values and those used in solving the direct problem, are effective. It has been established that the values of $\tilde{q}_0(\mathrm{Fo})$ calculated from ΔT in the case of convective heat fluxes correspond to the membrane zones with maximum temperatures, i.e., the information that can be obtained by Gardon-type sensors pertains to the zones with minimum heat fluxes. The results of the numerical experiment are also indicative of large errors in the intensity determination for the external thermal perturbation with use of standard calibrations characteristics under conditions of substantially nonsteady heat fluxes and on the initial sections of realization even for heat fluxes changing slightly in time.

Besides calculation of $\tilde{q}_0(\mathrm{Fo})$ by formula (18) the program developed included calculation of $\tilde{q}_0(\mathrm{Fo})$ by asymptotic approximation formulas that may be derived from estimates of the behavior of the inverse transforms at $\mathrm{Fo} \to \infty$ [4]. On the basis of these estimates, we have approximately

$$\tilde{q}_0(\mathrm{Fo}) \approx m_0 \Delta T(\mathrm{Fo}) + m_1 \frac{d\Delta T(\mathrm{Fo})}{d\mathrm{Fo}} + m_2 \int_0^{\mathrm{Fo}} (\mathrm{Fo} - \vartheta)^{-1/2} \frac{d\Delta T(\vartheta)}{d\vartheta}\, d\vartheta, \tag{19}$$

where

$$m_0 = \frac{4(1 + \varepsilon_2/\varepsilon_3 \overline{R}_0)}{\zeta} \frac{\lambda_1 \delta}{R_{\mathrm{in}}^2},$$

$$\zeta = (1 - \overline{R}_0^2)\left(1 + \frac{\varepsilon_2}{\varepsilon_3}\overline{R}_0\right) + 2\overline{R}_0\left(\overline{R}_0 + \frac{\varepsilon_2}{\varepsilon_3}\right)\ln \overline{R}_0;$$

$$m_1 = \frac{(1 - \overline{R}_0^2)(1 - \varepsilon_2/\varepsilon_3 \overline{R}_0) + 2\overline{R}_0(\overline{R}_0 - 4/\varepsilon_3 - \varepsilon_2/\varepsilon_3)\ln \overline{R}_0}{\zeta} \frac{\lambda_1 \delta}{R_{\mathrm{in}}^2};$$

$$m_2 = \frac{4}{\sqrt{\pi}} \frac{k_2^{-1/2} \gamma_2^{-1} [1 + \overline{R}_0 \varepsilon_2/\varepsilon_3 + 1/2\varepsilon_2/\varepsilon_3 (1 - \overline{R}_0^2)] - \frac{\overline{R}_0 \varepsilon_2}{\varepsilon_3} k_3^{1/2} \gamma_3 \ln \overline{R}_0}{\zeta} \frac{\lambda_1 \delta}{R_{\mathrm{in}}^2}.$$

Note that for $\Delta T' = 0$ and $\overline{R}_0 = 0$ the following relation holds:

$$\tilde{q}_0 = \frac{4\lambda_1 \delta}{R_{\mathrm{in}}^2} \Delta T = \tilde{k}_0 \Delta T,$$

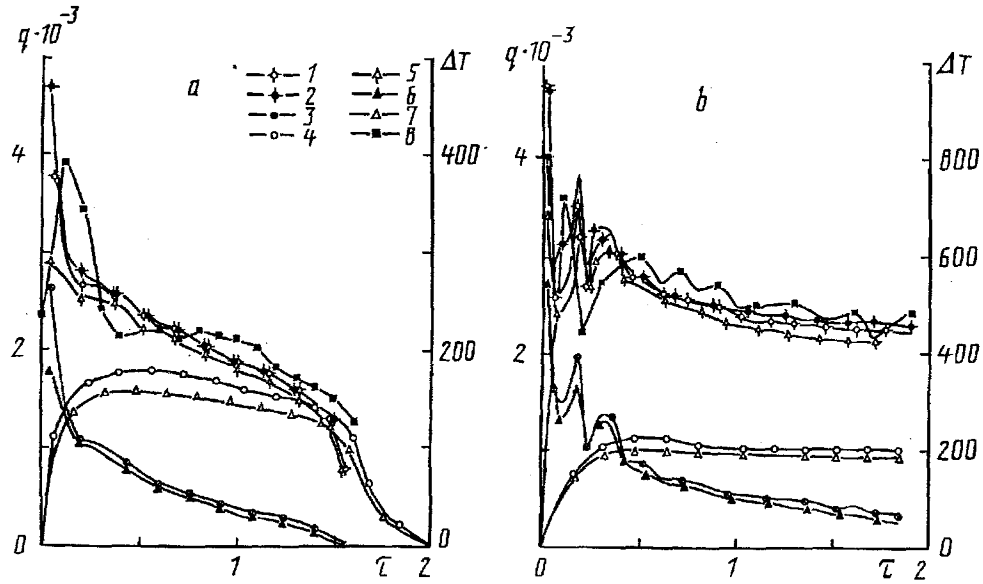

Fig. 2. Results of processing of the experimental data: 1-4) Constantan membranes; 5-7) Copel membranes; (1, 5) q calculated by the "exact" relations; 2) q calculated by the asymptotic approximation formulas; 3, 6) difference between the q values calculated by the exact relations and the readings of the Gardon sensors with standard calibration; 4, 7) output signal of the Gardon sensor (the temperature difference between the center of the membrane and the periphery); 8) results of evaluation of heat fluxes from the measurement data produced by wall-temperature sensors positioned in regions where Gardon sensors are placed. q, $kW \cdot m^{-2}$; ΔT, K; τ, sec.

where $\tilde{k}_0$ coincides with the theoretical calibration coefficient for Gardon-type sensors under steady conditions.

The results of the numerical experiment indicate that an approximate dependence of the form (19) yields reasonable, from a practical viewpoint, estimates of $\tilde{q}_0$ even for comparatively small Fo numbers and for rather nonsteady external heat transfer within the ranges of the dimensions, used in practice, of structural elements of the sensors and the thermophysical characteristics of the materials of the membrane and the electrodes.

Furthermore, the program of $\tilde{q}_0$(Fo) calculation was used for processing the measurement data obtained in comparative tests of Gardon sensors and temperature sensors of a metallic wall surface subjected to the action of high-temperature gas flows. In those tests the intensity of the thermal perturbation was determined using both the measured temperatures of the metallic wall surface and the Gardon sensors with standard calibration coefficients. A comparison of the information on heat fluxes obtained after processing the readings of the wall-temperature sensors and the data produced by the Gardon sensors revealed substantially different values of the heat fluxes in the two cases. The values produced by the Gardon sensors were much lower than those calculated from the surface temperatures of the measuring column of the wall-temperature sensor. This circumstance considered, we found it reasonable to correct the data of heat flux measurements by the Gardon sensors by using algorithms that take into account the nonsteady effects of temperature field formation in structural elements of the sensor.

In calculations, we adopted the following values of the thermophysical characteristics of the materials and the dimensions: $\lambda_m = 0.0242\ kW \cdot m^{-1} \cdot K^{-1}$, $c_m \rho_m = 2822.9\ kJ \cdot m^{-3} \cdot K^{-1}$ for a Copel membrane; $\lambda_m = 0.023\ kW \cdot m^{-1} \cdot K^{-1}$, $c_m \rho_m = 3640\ kJ \cdot m^{-3} \cdot K^{-1}$ for a Constantan membrane; $\lambda_e = 0.37\ kW \cdot m^{-1} \cdot K^{-1}$; $c_e \rho_e = 3221.6\ kJ \cdot m^{-1} \cdot K^{-1}$; $2R_0 = 0.5$ mm; $2R_{out} = 7$ mm; $2R_{in.} = 1.5$ mm; $\delta = 0.3$ mm. The calculations were made for two variants (Copel and Constantan) of the membranes because of the absence of reliable information on the kind of a material used in a particular sensor.

The results of $\tilde{q}_0(\text{Fo})$ calculation using the "exact" relations and an asymptotic approximation as well as the difference between the calculated $\tilde{q}_0(\text{Fo})$ values and those obtained with the aid of standard calibration characteristics of the sensor are demonstrated in Fig. 2. There, the results of heat flux calculations from the data of measurement by wall-temperature sensors are shown.

An analysis of the data in Fig. 2 enables us to draw the following conclusions. An account for nonsteady effects in processing the output signal of the Gardon sensor with use of the "exact" relation results in a substantial difference of the $\tilde{q}_0(\text{Fo})$ values from those recorded by the sensors (i.e., with use of the traditional approach: multiplication of the output signal in the form of an emf by a calibration coefficient), especially on the initial sections of realization and on the sections of abrupt changes in the time of the external thermal perturbations. The $\tilde{q}_0(\text{Fo})$ values calculated using the program developed become close (in the majority of cases) to the values obtained in processing the temperatures measured by the wall-temperature sensors. In addition, with the exception of very "short" initial sections of realization and very short intervals of time from the moment of drastic change in the external thermal perturbation, the $\tilde{q}_0(\text{Fo})$ values calculated by the asymptotic approximation formulas differ only slightly from those calculated by the exact relation. The latter circumstance is of importance from a practical viewpoint since a comparatively simple functional relationship between ΔT and $\tilde{q}_0$ makes it possible in this case to use a sufficiently simple algorithm of processing the output signal of the Gardon sensor for obtaining reliable data on an external thermal perturbation under substantially nonsteady thermal conditions.

Thus, analysis of the data of some numerical experiments and also the data of processing the temperature data obtained in a physical experiment enable us to conclude that significant errors may arise when sensors of the Gardon type are used in a traditional manner for obtaining information on intensities of incoming heat fluxes under conditions of short-term heating processes and significantly nonsteady convective heat transfer.

NOTATION

$\bar{r} = r/R_{in}$; $\bar{x} = x/R_{in}$; $\bar{z} = z/R_{in}$; $\text{Fo} = a_1\tau/R_{in}^2$; $\bar{q}(\bar{r}, \text{Fo}) = q(r, \text{Fo})R_{in}^2/\lambda_1\delta$; $\beta_1 = \frac{\alpha_1 R_{in}^2}{\lambda_1\delta}$; $\beta_2 = \frac{\alpha_2 R_{in}^2}{\lambda_2}\cdot\frac{\Pi_2}{f_2}$; $\beta_3 = \frac{\alpha_3 R_{in}^3}{\lambda_3}\cdot\frac{\Pi}{f_3}$; $\varepsilon_2 = \frac{f_{2,1}}{f_2}\cdot\frac{R_{in}}{\delta}$; $\gamma_2 = \frac{\lambda_2}{\lambda_1}\cdot\frac{R_{in}}{\delta}$; $\varepsilon_3 = \frac{f_{3,1}}{f_3}\cdot\frac{R_{in}}{\delta}$; $\gamma_3 = \frac{\lambda_3}{\lambda_1}\cdot\frac{R_{in}}{\delta}$; $\bar{h} = h/R_{in}$; $\bar{L} = L/R_{in}$; $k_2 = a_1/a_2$; $k_3 = a_1/a_3$; α_1, coefficient of heat transfer from the internal surface of the membrane; α_2, coefficient of heat transfer from the internal side surface of the electrode at the periphery; α_3, coefficient of heat transfer from the side surface of the central electrode; f_2, cross-sectional area of the electrode at the periphery; $f_2 = \pi(R_{out}^2 - R_{in}^2)$; f_3, cross-sectional area of the central electrode; $f_3 = \pi R_0^2$; $f_{2,1} = 2\pi R_{in}\delta$; $f_{3,1} = 2\pi R_0\delta$; $\Pi_2 = 2\pi R_{in}$; $\Pi_3 = 2\pi R_0$; λ_1, λ_2; λ_3, thermal conductivity of the material of the membrane, the electrode at the periphery, and the central electrode, respectively; a_1, a_2, a_3, thermal diffusivity of the material of the membrane, the electrode at the periphery, and the central electrode; $c_1\rho_1 = \lambda_1/a_1$; $c_2\rho_2 = \lambda_2/a_2$; $c_3\rho_3 = \lambda_3/a_3$; h, height of the electrode at the periphery; L, length of the central electrode. Subscripts: in, inner; out, outer; e, electrode; m, membrane.

REFERENCES

1. Striegle and Diller, Teploperedacha, No. 1, 25 (1984).
2. Borell and Diller, Teploperedacha, No. 1, 82-90 (1987).
3. A. M. Borob'ev, V. I. Zhuk, V. P. Sizov, and D. N. Chubarov, Inzh.-Fiz. Zh., 58, No. 2, 264-270 (1990).
4. A. V. Luikov, Theory of Heat Conduction [in Russian], Moscow (1967).
5. V. A. Ditkin and A. P. Prudnikov, Operational Calculus, Handbook, Moscow (1965).